Published June 11, 2007

Senataxin, defective in ataxia oculomotor apraxia type 2, is involved in the defense against oxidative DNA damage

Amila Suraweera,[1,2] Olivier J. Becherel,[1] Philip Chen,[1] Natalie Rundle,[1] Rick Woods,[1] Jun Nakamura,[3] Magtouf Gatei,[1] Chiara Criscuolo,[4] Alessandro Filla,[4] Luciana Chessa,[5] Markus Fußer,[6] Bernd Epe,[6] Nuri Gueven,[1] and Martin F. Lavin[1,2]

[1]Radiation Biology and Oncology Laboratory, Queensland Institute of Medical Research, Brisbane, QLD 4029, Australia
[2]Central Clinical Division, University of Queensland, Brisbane, QLD 4029, Australia
[3]Department of Environmental Sciences and Engineering, University of North Carolina at Chapel Hill, Chapel Hill, NC 27599
[4]Department of Neurobiology, University of Naples, Naples, 80131, Italy
[5]Department of Experimental Medicine and Pathology, University "La Sapienza," Roma, 324-00161, Italy
[6]Institute of Pharmacy, University of Mainz, Mainz, 55099, Germany

A defective response to DNA damage is observed in several human autosomal recessive ataxias with oculomotor apraxia, including ataxia-telangiectasia. We report that senataxin, defective in ataxia oculomotor apraxia (AOA) type 2, is a nuclear protein involved in the DNA damage response. AOA2 cells are sensitive to H_2O_2, camptothecin, and mitomycin C, but not to ionizing radiation, and sensitivity was rescued with full-length *SETX* cDNA. AOA2 cells exhibited constitutive oxidative DNA damage and enhanced chromosomal instability in response to H_2O_2. Rejoining of H_2O_2-induced DNA double-strand breaks (DSBs) was significantly reduced in AOA2 cells compared to controls, and there was no evidence for a defect in DNA single-strand break repair. This defect in DSB repair was corrected by full-length *SETX* cDNA. These results provide evidence that an additional member of the autosomal recessive AOA is also characterized by a defective response to DNA damage, which may contribute to the neurodegeneration seen in this syndrome.

Introduction

Ataxia-telangiectasia (A-T) represents a paradigm for several autosomal recessive ataxias characterized by defects in the recognition and/or repair of DNA damage (Lavin and Shiloh, 1997). The protein defective in A-T, A-T mutated (ATM), recognizes and is activated by DNA double-strand breaks (DSBs) to signal this damage to the cell cycle checkpoints and the DNA repair machinery (Kurz and Lees-Miller, 2004). Loss of ATM function results in hypersensitivity to ionizing radiation (IR), cell cycle checkpoint defects, genome instability, increased cancer incidence, and neurodegeneration (Hernandez et al., 1993). A-T–like disorder (A-TLD), as a result of hypomorphic mutations in the *MRE11* gene, most closely resembles A-T in its clinical phenotype (Taylor et al., 2004). Mre11 functions in a complex with Rad50 and Nbs1 (defective in Nijmegen breakage syndrome) to localize to sites of DNA DSB. This complex acts upstream of ATM in sensing DSB and ensures efficient activation of ATM (Uziel et al., 2003; Cerosaletti and Concannon, 2004; Lee and Paull, 2005). Once activated, ATM phosphorylates a series of substrates, including Nbs1, which acts as an adaptor molecule for control of the intra-S and G2/M cell cycle checkpoints (Uziel et al., 2003). A third syndrome, ataxia oculomotor apraxia (AOA) type 1, also overlaps in its clinical phenotype with A-T (Aicardi et al., 1988; Le Ber et al., 2003). Mutations in the *APTX* gene are responsible for this neurological disorder (Date et al., 2001; Moreira et al., 2001). Recent evidence shows that the protein mutated in this syndrome, aprataxin, plays a role in the repair of DNA single-strand breaks (SSBs; Clements et al., 2004; Gueven et al., 2004; Mosesso et al., 2005), possibly by resolving abortive DNA ligation intermediates (Ahel et al., 2006).

A distinct form of AOA linked to chromosome 9q34, AOA2 also has an overlapping clinical phenotype with the three disorders described in the previous paragraph (Nemeth et al., 2000; Duquette et al., 2005; Le Ber et al., 2005). This

A. Suraweera and O.J. Becherel contributed equally to this paper.

Correspondence to Martin F. Lavin: martin.lavin@qimr.edu.au

Abbreviations used in this paper: AOA, ataxia oculomotor apraxia; A-T; ataxia-telangiectasia; A-TLD, A-T–like disorder; ATM, A-T mutated; CPT, camptothecin; DSB, double-strand break; IR, ionizing radiation; MMC, mitomycin C; NFF, normal foreskin fibroblast; SSB, single-strand break.

The online version of this article contains supplemental material.

Supplemental Material can be found at:
http://jcb.rupress.org/content/suppl/2007/06/11/jcb.200701042.DC1.html

The Journal of Cell Biology, Vol. 177, No. 6, June 18, 2007 969–979
http://www.jcb.org/cgi/doi/10.1083/jcb.200701042

Published June 11, 2007

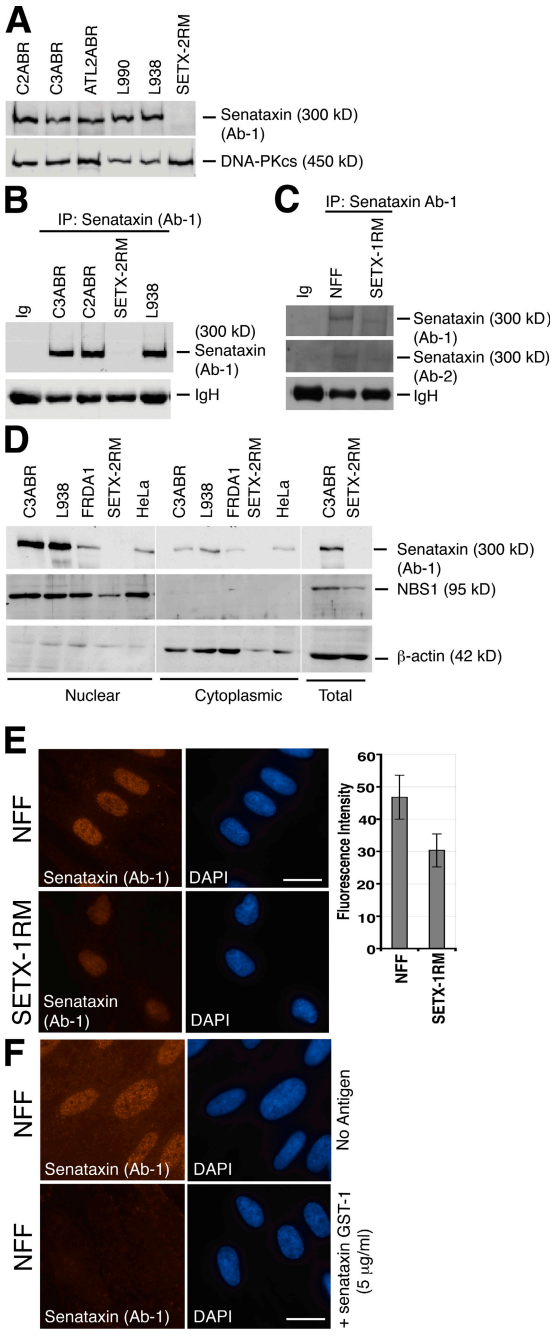

Figure 1. **Expression and localization of senataxin.** (A) Expression of senataxin in control (C2ABR and C3ABR), an unclassified AOA (ATL2ABR), AOA1 (L938, L939), and AOA2 (SETX-2RM) lymphoblastoid cells. Senataxin levels were measured in total cell extract by immunoblotting using Ab-1. DNA-PKcs is a loading control. (B) Immunoprecipitation of senataxin from C2ABR, C3ABR, L938, and SETX-2RM using Ab-1. Preimmune sera (Ig) was used as a negative control. IgH shows equal loading. (C) Immunoprecipitation of senataxin using Ab-1 from normal (NFF) and AOA2 (SETX-1RM) fibroblasts. Senataxin is detected by immunoblotting with both Ab-1 and Ab-2. IgH shows equal loading. (D) Nuclear and cytoplasmic extracts were made from C3ABR, L938, SETX-2RM, Friedrich's ataxia (FRDA1), and HeLa cells. Total cell extract from C3ABR and SETX-2RM are also shown. Senataxin levels are shown using Ab-1. NBS1 and β-actin were used to assess the purity of the fractions. (E) Cellular localization of senataxin by immunostaining of normal (NFF) and AOA2 (SETX-1RM) fibroblasts with Ab-1. DAPI shows nuclei. Fluorescence intensity from 50 individual cells for each NFF and SETX-1RM was quantitated using ImageJ software. Levels of senataxin in NFF and SETX-1RM are represented by the mean fluorescence intensity expressed in arbitrary units. SD was calculated from 50 measurements in each case. $P < 0.001$ (*t* test). (F) Confirmation of nuclear localization of senataxin using competition with antigen (senataxin GST-1), recognized by Ab-1, to inhibit binding in NFF cells. Bars, 20 μm.

syndrome is characterized by cerebellar atrophy, oculomotor apraxia, peripheral neuropathy, and elevated serum α-fetoprotein in some cases (Le Ber et al., 2005; Criscuolo et al., 2006). The gene defective in AOA2, *SETX*, was recently identified (Moreira et al., 2004). Mutations in *SETX* are also associated with an autosomal dominant, juvenile onset form of amyotrophic lateral sclerosis (Chen et al., 2004). Senataxin, the predicted protein encoded by *SETX* is 2,677 amino acids in length and contains a seven-motif domain at its C terminus, typical of the superfamily I of DNA/RNA helicases (Moreira et al., 2004). Senataxin has extensive homology to the *Schizosaccharomyces pombe* Sen1p proteins that possess helicase activity and are required for the processing of diverse RNA species that include transfer RNA, ribosomal RNA, small nuclear RNA, and small nucleolar RNA (Ursic et al., 1997). Sen1p proteins are also related to other DNA/RNA helicases, Upf1, involved in nonsense-mediated decay (Weng et al., 1996) and IGHMBP2, defective in a form of spinal muscular atrophy (Grohmann et al., 2001). Use of global and candidate-specific two-hybrid screens identified Rpo21p, a subunit of RNA polymerase II and Rnt1p, an endoribonuclease required for RNA maturation, as a Sen1p-interacting protein (Ursic et al., 2004), providing further support for a role in RNA processing. Recently, Steinmetz et al. (2006) showed that a single amino acid mutation that compromises Sen1 function in *Saccharomyces cerevisiae* altered the genome-wide distribution of RNA polymerase II, providing evidence for a role in transcription regulation. Interestingly, Sen1p was also shown to interact with Rad2p, a DNase required for nucleotide excision repair after DNA damage (Ursic et al., 2004). These observations on yeast orthologues, together with an overlapping phenotype with other autosomal recessive ataxias with oculomotor apraxia, which are characterized by defective DNA repair, led us to investigate whether senataxin might also play a role in the DNA damage response. We show here that senataxin is primarily a nuclear protein and that AOA2 cells have increased sensitivity to H_2O_2, camptothecin (CPT), and mitomycin C (MMC), but a normal response to IR, compared with controls. To determine whether senataxin was responsible for this cellular phenotype, we cloned full-length *SETX* cDNA and demonstrated complementation of agent sensitivity in stably transfected AOA2 cell lines. The increased sensitivity to H_2O_2 was associated with a defect in DNA DSB repair, but there was no defect in repair of SSBs or in DSBs produced by IR exposure. These results add further substance to the hypothesis that a defective DNA damage response contributes to the neurodegenerative phenotype in a subgroup of the autosomal recessive ataxias.

Results

Detection and subcellular localization of senataxin

Cell lines were established from two patients with AOA2, fibroblasts (SETX-1RM) and a lymphoblastoid cell line (SETX-2RM).

Published June 11, 2007

Identification of the mutations in *SETX* was performed by PCR followed by DNA sequencing. The results in Fig. S1 A (available at http://www.jcb.org/cgi/content/full/jcb.200701042/DC1) show that for SETX-1RM, a homozygous deletion of 1 kb occurred at the cDNA level as a result of a large deletion in genomic DNA, which resulted in the deletion of exons 14–21 of *SETX*. Mutation in *SETX* was also homozygous for SETX-2RM, involving exon 23 skipping because of a missense mutation at the splice site (IVS 23 + 5 G > A; Fig. S1 B).

To detect the presence of senataxin protein and investigate its subcellular localization, we produced two polyclonal antibodies against the C-terminal (Ab-1/Ab-3) and another against the N-terminal (Ab-2) regions of the protein (Fig. S2 A, available at http://www.jcb.org/cgi/content/full/jcb.200701042/DC1). Specificity of the antibodies was determined by dot blot analysis (Fig. S2, B–E). The two C-terminal antibodies reacted only with a GST fusion protein corresponding to this C-terminal region of the molecule (senataxin GST-1), whereas the N-terminal antibody specifically recognized this region of the molecule (senataxin GST-2). Preimmune serum failed to detect senataxin GST. The results in Fig. 1 A show that Ab-l detected the presence of a single prominent band at ~300 kD for two control cell lines (C2ABR and C3ABR), two AOA1 cell lines (L990 and L938), an unclassified AOA cell line (ATL2ABR) but was absent in an AOA2 cell line (SETX-2RM), as predicted from the exon-skipping mutation. The same pattern was observed with all three antibodies (unpublished data). Immunoprecipitation with Ab-1 followed by immunoblotting with the same antibody also detected a single band of the same size, which was again absent in the AOA2 cells (Fig. 1 B). Nonspecific antisera failed to immunoprecipitate senataxin. It was not possible to detect senataxin in primary fibroblasts with up to twofold increased protein loading by immunoblotting on total cell extracts (unpublished data). However, immunoprecipitation with Ab-1 followed by immunoblotting with two senataxin antibodies (Ab-1 and Ab-2) revealed the presence of senataxin in normal foreskin fibroblasts (NFFs; Fig. 1 C). This might be explained by a lesser amount present in the fibroblasts or a reduced relative amount of nuclear protein in fibroblasts compared with lymphoblasts. A slightly lower molecular size band for senataxin was detectable in an AOA2 fibroblast (SETX-1RM), consistent with the deletion of exons 14–21, which would maintain the reading frame but would lead to the loss of 322 amino acids (Fig. 1 C). Fractionation of cell extracts followed by immunoblotting with senataxin antibodies revealed that this protein was primarily a nuclear protein (Fig. 1 D). Senataxin was present in the cytoplasm but markedly reduced compared with that in the nucleus. It is notable that the amount of senataxin varied with cell type being highest in lymphoblastoid cells. Comparison of AOA2 (SETX-1RM) fibroblasts with NFFs (controls) using immunofluorescence demonstrated reduced nuclear staining in the AOA2 cells (Fig. 1 E). To confirm that the nuclear staining was specific, we performed competition experiments with antigen (senataxin GST-1) corresponding to a C-terminal peptide (Fig. 1 F). The results in Fig. 2 A confirm that senataxin, detected by both N- and C-terminal antibodies, is predominantly a nuclear protein and appears to be excluded from the nucleolus, as shown

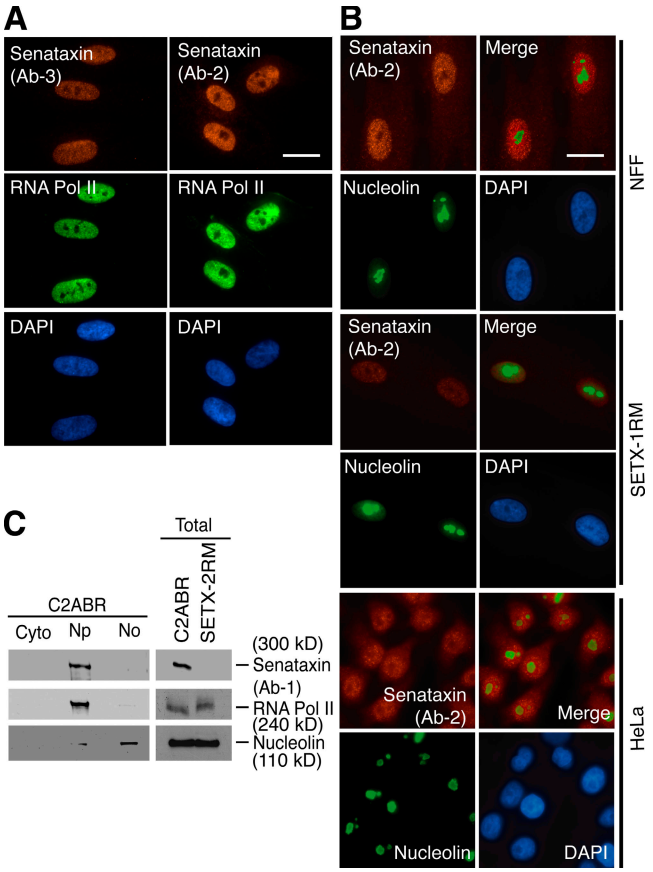

Figure 2. **Senataxin is a nucleoplasmic protein.** (A) Immunostaining for senataxin was performed in NFFs using both Ab-2 and Ab-3. RNA polymerase II identifies the nucleoplasm, and DAPI identifies the nucleus. (B) Senataxin does not localize to the nucleolus as shown by nonoverlapping staining pattern for senataxin and nucleolin, a specific marker of the nucleolus in NFFs, SETX-1RM, and HeLa. Bars, 20 μm. (C) Subcellular fractionation of control cells (C2ABR) was used to detect senataxin by immunoblotting using Ab-1. Cyto, cytoplasmic fraction; Np, nucleoplasmic fraction; No, nucleolar fraction. Detection of nucleolin and RNA polymerase II was used to determine the purity of the fractions. Total cell extract from C3ABR and SETX-2RM cells are also shown.

by a staining pattern similar to that of RNA polymerase II, a nucleoplasmic protein. Further support for this is provided by the failure of senataxin to colocalize with nucleolin in the nucleolus of NFFs or HeLa cells (Fig. 2 B). This was also the case for SETX-1RM fibroblasts, which contain a truncated form of senataxin. Finally, evidence that senataxin is predominantly a nucleoplasmic protein was provided by subcellular fractionation and immunoblotting (Fig. 2 C). Under these conditions, a prominent senataxin band was detected in the nucleoplasm but not in the nucleolus or cytoplasm. Immunoblotting for RNA polymerase II and nucleolin was performed to demonstrate the integrity of the cellular fractions (Fig. 2 C).

Sensitivity of AOA2 cells to DNA damaging agents and complementation of the defect

Because it has been demonstrated that cell lines from patients with other autosomal recessive ataxias, which overlap in their clinical phenotype with AOA2, are sensitive to DNA damaging

Published June 11, 2007

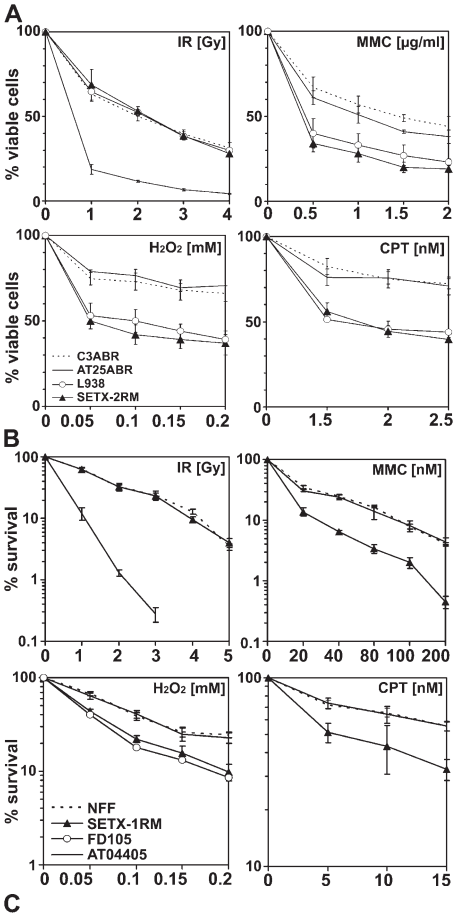

C

Cell line	Sb	Cb	Int	ICA/cell
C3ABR	101	1	0	2.04 ± 0.07
SETX-2RM	210	0	0	4.20 ± 0.13

Sb, chromatid breaks; Cb, chromosome breaks; Int, Interchange; ICA, induced chromosome aberrations. Fifty metaphases were analyzed for each sample after exposure to 2mM H_2O_2.

Figure 3. **Sensitivity of AOA2 cells to DNA damaging agents.** (A) Cell viability of control (C3ABR), A-T (AT25ABR), AOA1 (L939), and AOA2 (SETX-2RM) lymphoblastoid cells after treatment with the genotoxic agents (IR, MMC, H_2O_2, and CPT) was determined by Trypan blue staining. (B) Cell survival of normal (NFF), A-T, (AT04405) AOA1 (FD105), and AOA2 (SETX-1RM) fibroblasts after IR, MMC, CPT, and H_2O_2 treatments. Cell survival was determined by counting fibroblast colonies. *t* test analysis demonstrated a significant difference between NFF and SETX-1RM with P values of 0.008 at 0.05 mM, 0.017 at 0.1 mM, 0.014 at 0.15 mM, and 0.03 at 0.2 mM of H_2O_2. Error bars indicate SD. (C) Chromosome aberrations induced in response to exposure to 2 mM H_2O_2 for 30 min.

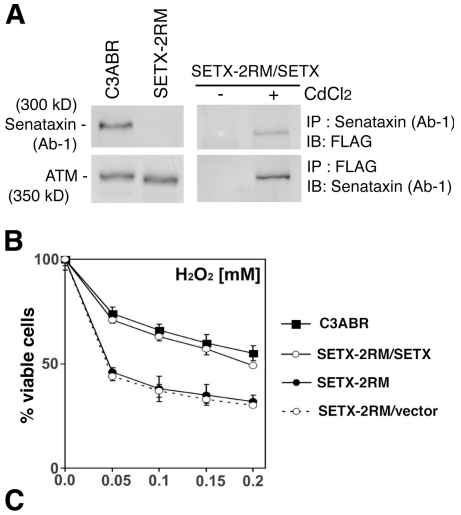

C

Cell line	Sb	Cb	Int	ICA/cell
C3ABR	106	0	0	2.12 ± 0.08
SETX-2RM	211	0	0	4.22 ± 0.10
SETX-2RM/SETX	109	0	0	2.18 ± 0.07
SETX-2RM/vector	197	1	0	3.96 ± 0.11

Sb, chromatid breaks; Cb, chromosome breaks; Int, Interchange; ICA, induced chromosome aberrations. Fifty metaphases were analyzed for each sample after exposure to 2mM H_2O_2 for 30 min in aerobic conditions.

Figure 4. **Complementation of H_2O_2 cell sensitivity and induced chromosome aberrations with *SETX* cDNA.** (A) Induction of senataxin by $CdCl_2$ in SETX-2RM cells transfected with full-length *SETX* cDNA. Senataxin expressed in the presence of $CdCl_2$ was detected by immunoprecipitation with anti-senataxin followed by immunoblotting with anti-FLAG antibody or by reversing the antibody combination. (B) Complementation of cell survival of SETX-2RM lymphoblastoid with full-length *SETX*. Empty vector (SETX-2RM/Vector) was used as a negative control. Error bars indicate SD. (C) Complementation of H_2O_2-induced chromosome aberrations in SETX-2RM using full-length *SETX* cDNA.

agents, we determined whether this might also be the case for AOA2. The results in Fig. 3 A reveal that AOA2 lymphoblastoid cells (SETX-2RM) show a normal pattern of sensitivity to IR but have increased sensitivity to H_2O_2, CPT, and MMC, compared with controls. AOA1 cells are also sensitive to H_2O_2, as we have previously shown (Gueven et al., 2004). A-T cells showed normal sensitivity to these DNA damaging agents but hypersensitivity to IR. Increased sensitivity was also observed with H_2O_2, MMC, and CPT in AOA2 fibroblasts (Fig. 3 B). Although these agents give rise to either cross-links or SSBs and DSBs in DNA, there is also evidence that their toxicity is associated with redox-related pathways (Pagano et al., 2005). AOA1 fibroblasts were also sensitive to H_2O_2 (Fig. 3 B). As an additional measure of sensitivity, we compared the levels of H_2O_2-induced chromosome aberrations. The results in Fig. 3 C reveal approximately two induced chromosome aberrations per metaphase in H_2O_2-treated control cells, whereas a further two-fold increase was observed in AOA2. To demonstrate that the increased sensitivity to H_2O_2 was due to loss of senataxin, we cloned full-length *SETX* cDNA into the Epstein-Barr virus–based expression vector pMEP4, containing a FLAG tag sequence, and established stable cell lines as previously described (Zhang et al., 1997). DNA sequencing detected five polymorphic changes in *SETX* and three nonconserved amino acid changes compared with the sequence in the database (available from GenBank/EMBL/DDBJ under accession no. AB014525). This construct, pSETX1, contains a metallothionein promoter, which allows inducible expression of senataxin by $CdCl_2$. Induction of senataxin was detected by immunoprecipitation with anti-senataxin and anti-FLAG antibodies followed by immunoblotting with the respective antibodies (Fig. 4 A, right). Immunoblotting on total cell extracts confirmed that AOA2 (SETX-2RM) parental cells lack senataxin as compared with control cells (Fig. 4 A, left). Exposure of *SETX*-transfected AOA2 cells to H_2O_2 after induction of senataxin corrected the H_2O_2 hypersensitivity in these cells (Fig. 4 B). On the other hand, AOA2 cells transfected with empty vector remained hypersensitive to H_2O_2. *SETX* cDNA also corrected the H_2O_2-induced

Published June 11, 2007

chromosome aberrations in AOA2 cells (Fig. 4 C), whereas vector alone did not change the number of aberrations.

Constitutive oxidative DNA damage in AOA2 cells

Because AOA2 cells were sensitive to H_2O_2, CPT, and MMC, all of which are capable of generating oxidative stress (Pagano et al., 2005), we investigated whether there might be an inherent defect in coping with oxidative damage in these cells. The presence of 8-oxo-deoxyguanosine (8-oxo-dG) was determined as a marker of reactive oxygen species–mediated DNA damage (Cooke et al., 2000). The results in Fig. 5 A reveal a high basal level of 8-oxo-dG in AOA2 fibroblasts (SETX-1RM), but not in controls (NFFs). Quantitation of 8-oxo-dG fluorescence intensity reveals an approximately twofold increase in AOA2 cells compared with controls (Fig. 5 B). Exposure of cells to H_2O_2 caused an increase in 8-oxo-dG in both controls and AOA2, but the extent of staining remained higher in the AOA2 cells (Fig. 5, A and B). To determine whether this represented more general oxidative damage in AOA2 cells or a defect at the level of DNA, we also assayed for protein nitrotyrosination and lipid peroxidation. The results showed background levels for both 3-nitrotyrosine and 4HNE-Michael adducts in AOA2 cells similar to those observed in normal fibroblasts, suggesting that these cells were not undergoing generalized oxidative stress (Fig. 5, C and D).

Repair of oxidative damage to DNA

Given that AOA2 cells were sensitive to agents that cause oxidative stress, and because these cells had evidence of constitutive oxidative DNA damage, we investigated their DNA repair capacity. For DNA SSB repair, we used alkaline elution analysis. Using this assay, we failed to observe any difference between control and AOA2 cells over a time course of 1-h repair (Fig. 6 A). These results were confirmed by determining intracellular NAD(P)H levels, which represents a reliable method to monitor imbalance in break repair in cells (Nakamura et al., 2003). Again, in this case, there was no evidence for a defect in the extent or duration of DNA single-strand breakage (Fig. 6 B).

H_2O_2 is also capable of inducing DSBs in DNA (Dahm-Daphi et al., 2000). To detect DSBs arising in DNA as a result of oxidative damage and eliminate those that occur as a consequence of DNA replication fork movement across a site of damage, cells were grown to confluency. DNA DSBs were detected by measuring H2AX phosphorylation visualized as foci at sites of DNA damage, a quantitative assessment for the appearance and repair of DNA DSBs (Rothkamm and Lobrich, 2003). Approximately equal numbers of γH2AX foci were detected in control and AOA2 cells between 10 and 50 min after treatment with H_2O_2 (Fig. S3, available at http://www.jcb.org/cgi/content/full/jcb.200701042/DC1), and in both cases, these foci coincided with MDC1 foci, further supporting that they were sites of DNA DSB (Fig. 7 A). However, the extent of disappearance of these foci appeared to be slower in AOA2 cells at 8 h after treatment than in controls (Fig. 7 A). Quantitation of these results showed that there was a significant difference between AOA2 and controls at 4, 6, and 8 h after treatment. By 8 h after treatment, 10% of the foci remained in control nuclei compared with

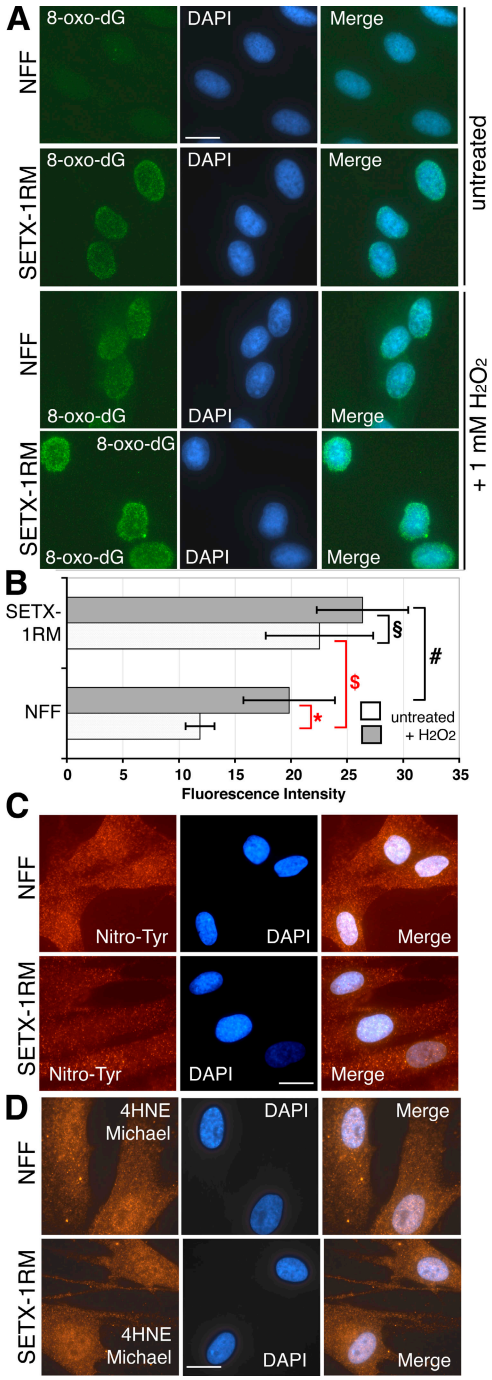

Figure 5. **Evidence for oxidative damage in AOA2 fibroblasts.** (A) Immunofluorescence detection of 8-oxo-dG levels in normal (NFF) and AOA2 (SETX-1RM) fibroblasts either untreated or treated with 1 mM H_2O_2 for 30 min in aerobic conditions. After treatment, H_2O_2-containing media was replaced with fresh media and cells were incubated for an additional 2 h before fixation and 8-oxo-dG detection. (B) Fluorescence intensity was quantitated on >50 individual cells for each treatment using ImageJ software. *t* test analysis demonstrated a significant difference in 8-oxo-dG levels in untreated NFFs and SETX-1M (*, $P < 0.001$) and NFFs untreated and treated with H_2O_2 ($, $P < 0.001$). No significant difference between H_2O_2-treated NFFs and SETX-1RM (#, $P = 0.5$) and SETX-1RM untreated and H_2O_2 treated (§, $P = 0.5$) was observed. Error bars indicate SD. (C) 3-nitrotyrosine (Nitro-Tyr) staining was used to examine the status of oxidative protein damage. (D) 4-hydroxy-2-noneal (4HNE)-Michael adducts were determined to assess the levels of lipid peroxidation. DAPI shows the nuclei. Bar, 20 μm.

Published June 11, 2007

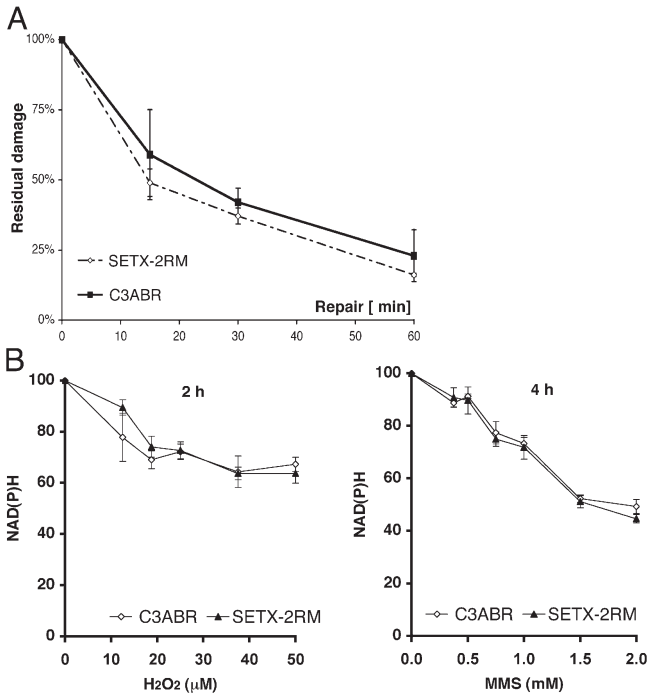

Figure 6. **DNA strand break repair in AOA2 cells.** (A) SSB repair of control (C3ABR) and AOA2 (SETX-2RM) cells in response to H_2O_2-induced DNA damage measured by alkaline elution at the indicated times after treatment. SSBs were induced by treating the cells with 20 μM H_2O_2 for 15 min at 37°C. (B) Measure of intracellular NAD(P)H depletion in response to H_2O_2 and methyl methanesulfonate (MMS) treatment was also used to determine appearance of SSBs in DNA. Error bars indicate SD.

39% in AOA2 cells, indicating a defect in repair of DSBs (Fig. 8 A). To determine whether this was a general defect in repair of DSBs, cells were exposed to IR, and the rate of disappearance of γH2AX foci was measured (Fig. 7 B). No difference in the rate of DSB repair after IR was observed (Fig. 8 B). The reduced capacity of AOA2 cells to repair the DSB induced by H_2O_2 does not appear to be explained by a trivial reason, such as widespread oxidative damage to proteins after incubation with H_2O_2 in the form of nitrotyrosinated proteins, as there was no evidence of gross damage (Fig. 5 C). To investigate further whether senataxin played a direct role in the DNA damage response, we performed transient transfections of AOA2 cells with *SETX*-GFP cDNA and assayed for correction of the DNA DSB defect after H_2O_2 treatment. Use of the *SETX*-GFP construct allowed us to differentiate between transfected and untransfected cells, providing an internal control for scoring of γH2AX foci. The results in Fig. S4 A reveal that the number of γH2AX foci are comparable in unlabeled and GFP-labeled cells. However, by 8 h after treatment, the number of γH2AX foci in GFP-labeled cells is significantly lower than that of γH2AX foci in nontransfected cells (Fig. S4 B). Similar experiments in transfected control fibroblasts revealed that the number of γH2AX foci was the same in unlabeled and GFP-labeled cells at 30 min after treatment with H_2O_2, and both cell types efficiently repaired the DNA DSBs by 8 h (Fig. S4, C and D). Foci were counted in at least 50 GFP-transfected and unlabeled cells and quantitated to reveal that *SETX*-cDNA corrected the DSB defect in AOA2 cells. These data appear in Fig. 8 A, indicating that full-length cDNA corrects the DNA DSB defect in AOA2 cells.

Discussion

Antibodies directed against both extremities of senataxin detected a protein of ∼300 kD, the predicted size from the reported open reading frame (Moreira et al., 2004). This protein was not detected in AOA2 lymphoblastoid cells with a mutation in *SETX* predicted to give rise to a prematurely truncated protein, but was detected as a lower molecular size form in fibroblasts (SETX-1RM) where an in-frame deletion was observed. We also provided firm evidence that senataxin is a nuclear protein with only minimal amounts in the cytoplasm. This protein is diffusely distributed throughout the nucleus with no evidence of localization to any subnuclear compartments. This is in contrast to a recent report demonstrating that senataxin was diffusely present in the cytoplasm and in the nucleolus in cultured cells (Chen et al., 2006). These data suggested that senataxin was expressed strongly in the cytoplasm in primate deep cerebellar nucleus but dull and diffuse in the nucleus. Using three different antibodies directed against both termini of senataxin, we showed diffuse nuclear labeling by immunofluoresence, which is supported by immunoblotting, revealing predominantly nuclear localization of the protein. We did not detect any senataxin in the nucleolus using either immunofluoresence or subcellular fractionation. It is of interest that Chen et al. (2006), using an N-terminal FLAG-tagged *SETX* construct, demonstrated only strong immunoreactivity throughout the nucleoplasm with an anti-FLAG antibody, in contrast to the results obtained with their anti-senataxin antibody. The authors interpreted this to mean that FLAG-senataxin is mislocalized. On the contrary, our data suggest that this is the correct localization.

Similar to that observed in A-T, A-TLD, and AOA1 cells, AOA2 cells are also characterized by sensitivity to DNA damaging agents. A-T cells are hypersensitive to IR and radiomimetic agents that give rise to DSBs in DNA (Taylor et al., 1975; Chen et al., 1978). A-TLD cells are also sensitive to these agents but not to the same extent as A-T (Stewart et al., 1999). The pattern of sensitivity described for AOA1 cells overlaps with that reported here for AOA2 (Gueven et al., 2004; Mosesso et al., 2005). Both cell types show increased sensitivity to H_2O_2, CPT, and MMC, but are not sensitive to IR. All three agents to which AOA2 cells are sensitive can give rise to DNA SSBs, but we found no evidence for a defect in SSB repair in AOA2. On the other hand, there is some evidence that AOA1 cells have a defect in SSB repair (Mosesso et al., 2005; Gueven et al., 2007), which is compatible with a role for aprataxin in resolving abortive DNA ligation intermediates (Ahel et al., 2006). Thus, the basis for the sensitivity to these agents appears to differ in AOA1 and AOA2 cells. The toxicity of these agents (MMC, CPT, and H_2O_2) is also associated with redox-related pathways (Pagano et al., 2005). A common observation in neurodegenerative disorders associated with DNA repair/signaling defects is an increase of spontaneous oxidative damages (Hayashi et al., 2001; Barzilai et al., 2002). Investigation of oxidative stress markers in AOA2 cells revealed higher basal levels of oxidative DNA damage

Published June 11, 2007

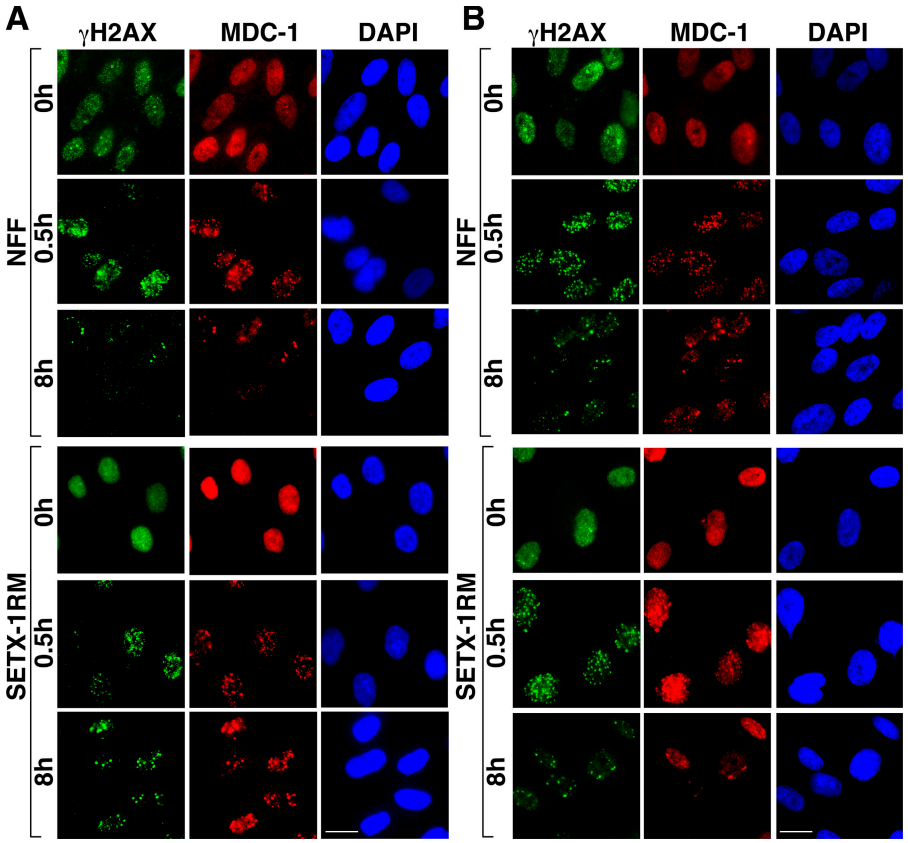

Figure 7. **DNA damage–induced γH2AX and MDC1 foci in NFFs and AOA2 (SETX-1RM) fibroblasts.** (A) H_2O_2-induced foci at 30 min and 8 h after treatment in control and AOA2 cells. (B) IR-induced foci at 30 min and 8 h after irradiation in control and AOA2 cells. Bars, 20 μm.

(8-oxo-dG) compared with controls, suggesting a reduced capacity to repair this type of DNA lesion (Hoffmann et al., 2004). This is further supported by a failure to observe more general oxidative damage in these cells.

At a higher concentration, H_2O_2-induced DSBs are also detected in DNA, as determined by the formation of γH2AX foci (Chen et al., 2005). They described the appearance of γH2AX foci in H_2O_2-treated cells after 2 h, which gradually decreased over 24 h. Coincidence was demonstrated between γH2AX and 53BP1 foci, providing additional evidence that these were DNA DSBs. In this study, we revealed a coincidence between γH2AX and MDC1 foci, a γH2AX-interacting protein that bridges the binding of the DNA damage response machinery to sites of DNA breaks (Stucki and Jackson, 2006). In the present study, these foci occurred to the same extent in both control and AOA2 cells in response to H_2O_2 treatment. However, the rate of loss of γH2AX foci was significantly reduced in AOA2 cells compared with controls from 4–8 h after treatment. The presence of high constitutive levels of 8-oxo-dG in AOA2 cells did not affect the number of breaks introduced into DNA by H_2O_2, but it is possible that these lesions might interfere with the rate of repair of the DSBs. An alternative but less likely explanation for the persistence of γH2AX foci in AOA2 cells is that these foci are indicative of aberrant chromatin structure by inappropriate rejoining of DNA breaks. Suzuki et al. (2006) provided this as an explanation to account for the persistence of γH2AX foci at a time when all the breaks were repaired on mitotic chromosomes. The defect in repair to DSBs was not a general one because AOA2 cells were as efficient as controls in repairing breaks induced by IR. These results suggest that the nature of the breaks is different after H_2O_2 and IR exposure. DNA damage caused by oxidation is complex and is deposited along the DNA molecule as single alterations or in clusters termed multiple DNA damage sites (Letavayova et al., 2006). This damage is primarily oxidized base damage and, when present at close proximity on opposite strands, can give rise to abortive base excision repair that leads to the formation of DNA DSBs (Wallace, 2002).

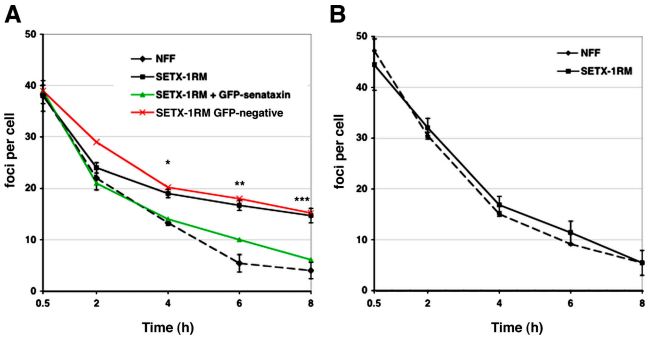

Figure 8. **Repair kinetic of DNA DSBs.** (A) Quantitation of γH2AX foci in control and AOA2 cells with time after incubation with H_2O_2. Greater than 90% of cells had foci, and quantitation was based on >100 cells/sample in repeat experiments. *t* test analysis demonstrated a significant difference between NFF and SETX-1RM: *, P = 0.02; **, P = 0.003; ***, P = 0.0008. Transient transfection of GFP-*SETX* cDNA into AOA2 cells (green) corrected the DSB repair defect as compared with GFP-negative cells (red). (B) Quantitation of γH2AX foci in control and AOA2 cells with time after exposure of cells to 2 Gy IR. Foci were quantitated as described in A. No significant difference in the repair kinetic of γH2AX foci was observed between NNFs and SETX-1RM after IR.

Published June 11, 2007

What distinguishes a DSB resulting from IR or H_2O_2 treatment? There is no easy answer to this, but it is evident that a DNA DSB arising from IR is efficient in attracting the Mre11 complex, activating ATM and the components of DNA repair (Bakkenist and Kastan, 2003; Kozlov et al., 2006). On the other hand, H_2O_2 is less efficient in activating ATM (Ismail et al., 2005; unpublished data). Furthermore, PDGFβ receptor transactivation acts as an upstream mediator of ATM kinase stimulation in response to H_2O_2 and, under these conditions, p53 is phosphorylated only on Ser15 (Chen et al., 2003). These data suggest that the mechanism of activation of ATM by IR and H_2O_2 are different and provide support for a difference in the nature of the DNA DSB generated in each case. Further support for a difference in the nature of the damage inflicted by H_2O_2 and IR is demonstrated by a lack of correlation in sensitivity to these agents in different cell lines (Cantoni et al., 1989; Bouzyk et al., 2000; Gueven et al., 2004) and difference in mutagenesis capacity (Gustafson et al., 2000) and in their effects on cell cycle progression (Wharton, 1995). Thus, it is not inconceivable that senataxin plays a specific role only in the processing of breaks generated by oxidative DNA damage.

It appears from the shape of the DNA repair curve that the initial rate of removal of breaks is comparable in control and AOA2 and that the defect is in a slower component of repair. This could be explained by a defect in repairing a subgroup of DNA breaks arising as a consequence of oxidative damage. 8 h after treatment with H_2O_2, 10% of breaks remained unrepaired in control cells, whereas almost four times as many (39%) were still detected in AOA2 cells. The subgroup of breaks may relate to double-strand ends with damaged termini. Although it is likely that •OH generated from H_2O_2 is responsible for much of the damage, there is also evidence for metal-mediated DNA damage, which is not protected against with hydroxyl radical scavengers (Li et al., 1999). Although Artemis-dependent processing of a subgroup of DNA breaks in response to radiation damage has been reported (Riballo et al., 2004), it is unlikely that the involvement of senataxin is in the ATM–Artemis pathway because DSBs induced by IR are normally repaired in AOA2.

The predicted protein sequence of senataxin contains a seven-helicase motif near its C terminus related to that present in the helicase superfamilies I and II (Gorbalenya et al., 1989), which play essential roles in maintaining genome integrity through their involvement in DNA replication, transcription, recombination, and repair (Hickson, 2003). Two members of the RecQ helicase family, WRN and RECQL4, mutated in Werner syndrome and Rothmund-Thompson syndrome, respectively, also protect against oxidative DNA damage (Szekely et al., 2005; Werner et al., 2006). The increased sensitivity to agents that cause oxidative stress and the reduced DSB repair in response to H_2O_2 exposure in AOA2 cells might also be explained by a defect in a helicase. However, although senataxin is an orthologue of yeast DNA/RNA helicases, no such activity has yet been demonstrated for this protein. A recent report by Steinmetz et al. (2006) showed that the yeast Sen1 helicase controlled the genome-wide distribution of RNA polymerase II, and a mutation that affected the function of this helicase led to profound changes in polymerase II distribution over noncoding and protein-coding genes, suggesting that Sen1 has an important role in control of gene expression. Given the similarity between the yeast and human Sen1 proteins, they suggested that mutations in senataxin may also lead to misregulation of transcription and in turn account for the progressive neurological defect in this syndrome. If it were to emerge that senataxin plays a similar role to yeast Sen1 in mammalian cells, it is not immediately evident how the transcriptional misregulation might account for some of the cellular characteristics that are described here for AOA2. Mouse cells lacking the WRN helicase exhibit altered expression of genes responding to oxidative stress (Deschenes et al., 2005). Furthermore, combining the defect with abrogation of the DNA repair gene poly (ADP-ribose) polymerase-1 (PARP-1) increased the extent of misregulation of gene expression. Aberrant transcription, chronic cellular stress, and apoptosis have also been suggested to contribute to the phenotype in Alzheimer's disease (Toiber and Soreq, 2005). The appearance of oxidative stress in AOA2 as described here could thus be explained by misregulation of transcription. Failure to respond normally to DNA damage and repair DSBs arising as a result of oxidative DNA damage might also be explained by the down-regulation of specific genes that are important for this process. Alternatively, as senataxin is a large protein characterized by only one putative helicase domain, it is possible that it has other activities or controls other proteins through interaction. Being able to reconcile the AOA2 cellular characteristics described here with a possible defect in regulation of gene expression requires a greater understanding of the functioning of this protein.

Materials and methods

Cell lines, survival, and induced chromosome aberrations

Lymphoblastoid cell lines (LCLs) from control (C3ABR and C2ABR), AOA1 (L938 and L939), Friedrich's ataxia (FRDA1), and AOA2 (SETX-2RM) patients were cultured in RPMI 1640 medium (Invitrogen) containing 10% FCS (JRH Biosciences), 2 mM L-glutamine (Life Technologies), 100 U/ml penicillin (Invitrogen), and 100 U/ml streptomycin (Invitrogen), and maintained in a humidified incubator at 37°C/5% CO_2. Fibroblasts from an AOA2 patient (SETX-1RM), NFFs (a gift from P. Parsons, Queensland Institute of Medical Research, Queensland, Australia), and HeLa were cultured in DME medium (Invitrogen) containing 10% FCS. LCLs were used at a density of 1×10^6 cells/ml, and adherent cells were used at 75% confluency except in the case of γH2AX foci experiments, where confluent cells were used. MMC, CPT, and H_2O_2 were purchased from Sigma-Aldrich. Irradiations were performed at room temperature using a ^{137}Cs source (Gammacell 40 Exactor [MDS Nordion]; dose rate 1.1 Gy/min). Lymphoblastoid cell viability (triplicate wells for each drug concentration) was measured by adding 0.1 ml of 0.4% trypan blue to 0.5 ml of cell suspension. The number of viable cells was counted, and viabilities were expressed as the number of cells in drug-treated wells relative to cells in untreated wells (percentage of viable cells), as previously described (Chen et al., 1978). The cells were incubated with the genotoxic agents for 1 h (MMC), 3 h (CPT), and 30 min (H_2O_2) before washing twice with PBS and suspension in culture medium. The number of viable cells was counted daily up to 4 d after treatment, and viability was calculated as described. The conditions were the same for fibroblasts, but survival was determined by colony formation. Cells were left for 2–3 wk to form colonies before staining with methylene blue and counting. Chromosomal aberrations were determined by treating cells with 2 mM H_2O_2 for 30 min in media under aerobic conditions. Colcemid (final concentration 0.1 μg/ml) was added immediately after treatment, 2 h before harvesting. The cells were treated for 15 min in 0.0075 M KCl and fixed in methanol ± glacial acetic acid (3:1), and the fixed cells were spread onto glass slides, air-dried, and stained with Giemsa. 50 metaphases were analyzed for each sample.

Published June 11, 2007

Cloning and expression of senataxin antigens

To produce senataxin antibodies, two regions of *SETX* were PCR amplified and cloned into bacterial expression vectors. In brief, a region of 450 bp of human *SETX* cDNA was PCR amplified from the 3′ end of senataxin using Ab-1F/Ab-1R primer pair. This *SETX* fragment was subsequently cloned into NheI and NotI sites of pTYB1 plasmid (New England Biolabs, Inc.), containing a C-terminal chitin binding domain. A second region of 1.1 kb of *SETX* was PCR amplified from the 5′ end of senataxin using Ab-2F/Ab-2R primer pair. The 5′ *SETX* fragment was cloned into EcoRI and NotI sites of pGEX-5X-1 plasmid (GE Healthcare), containing an N-terminal GST tag. Both of these constructs were transformed into *Escherichia coli* BL21 (DE3) pLysE cells, and overexpression was induced using 0.3 mM IPTG.

Production and purification of anti-senataxin antibodies

To produce senataxin antibodies, two regions of *SETX* corresponding to the N and C termini of the protein were PCR amplified, cloned into bacterial expression vectors, and transformed into *E. coli* (BL21 [DE3] pLysE). N- and C-terminal fusion proteins were affinity purified using chitin beads and glutathione–Sepharose resin, respectively, using the manufacturer's protocol. Sheep or rabbits were inoculated with senataxin antigens, and polyclonal antibodies were generated against the C (Ab-1/Ab-3) and N termini (Ab-2) of human senataxin using methods described previously (Bar-Peled and Raikhel, 1996). Senataxin antibodies were affinity purified using a series of GST-only and GST-N-ter/GST-C-ter columns.

Cloning of full-length *SETX* cDNA

Full-length *SETX* was PCR amplified and cloned into KpnI–NotI digested pMEP4 (see the supplemental text, available at http://www.jcb.org/cgi/content/full/jcb.200701042/DC1). For complementation studies, expression of senataxin was induced or mock-induced from pMEP4-transfected cells with 5 μM $CdCl_2$. *SETX* was also cloned into pEGFP-C2 by applying full-length *SETX* cDNA from pSPORT1_Sfi (RZPD Deutsches Ressourcenzentrum). *SETX*-GFP was used in transient transfection experiments.

PCR primers were designed to amplify two *SETX* fragments overlapping a unique SphI restriction site located at position 4432. Primer pairs HEF1/HER2 amplified a 5′ region from 1 to 4,375 bp and HEF3/HER3 amplified a 3′ region from 4,131 to 8,038 bp. PCR amplification was performed with 100 ng C3ABR cDNA, 1 μg of each primer, 100 μM dNTP, 1 × buffer 3, and 5 U *Taq* (Expand high fidelity *Taq*; Roche). Thermal cycling was performed in a PE-9700 PCR machine with the following settings: 95°C for 2 min, 30 cycles of 95°C for 30 s, 65°C for 30 s, and 6 min at 72°C. After amplification, DNA were purified on agarose gels. PCR fragments were subsequently A-tailed and cloned into pGEM-T-Vector (Promega). The 4-kb 3′ senataxin fragment was excised with SphI and SphI (pGEM-T vector site) and cloned into the 5′ SphI–SphI (pGEM-T vector site) restriction sites. After screening for correct orientation, the resulting full-length *SETX* cDNA clone was called pSETX. For expression of senataxin, the full-length senataxin cDNA was amplified from pSETX with Pfu Turbot *Taq* (Stratagene) using HEF5/HER5 primer pair, and the resulting product was cloned into KpnI–NotI digested pMEP4. The resulting pMEP4-*SETX* construct is referred to as pSETX1.

Detection of 8-oxo-dG by immunofluorescence

Cells on coverslips were fixed with 100% prechilled methanol for 5 min and immersed in 100% prechilled acetone for 5 min. Coverslips were subsequently air-dried, treated with 0.05 N HCl for 5 min on ice, and washed three times with PBS. RNA was digested by incubating the coverslips in 100 μg/ml RNase in 150 mM NaCl with 15 mM sodium citrate for 1 h at 37°C. After RNA digestion, coverslips were sequentially washed in PBS, 35, 50, and 75% ethanol for 2 min each. DNA was denatured by incubating the coverslips with 0.15 N NaOH in 70% ethanol for 4 min. A series of washes was performed starting with 70% ethanol containing 4% vol/vol formaldehyde and then 50% ethanol, 35% ethanol, and finally PBS for 2 min each. Proteins were digested with 5 μg/ml proteinase K in TE, pH 7.5, for 10 min at 37°C. After several PBS washes, coverslips were incubated with anti-8-oxo-dG antibody (1:250; 4355-MC-100 [Trevigen]) in PBT20 (1× PBS/1% BSA/0.1% Tween 20) for 1 h at room temperature. After several washes with 0.1× PBS, 8-oxo-dG was detected using an Alexa Fluor 488 secondary antibody (1:500 in PBT20; Invitrogen). Nuclei were counterstained with DAPI, and slides were mounted for immunofluorescence.

Cellular fractionation, immunoprecipitation, and immunoblotting

Cells were separated into cytoplasmic, nucleoplasmic, and nucleolar fractions as previously described (Scherl et al., 2002). For immunoprecipitations, cells were washed in PBS and resuspended in lysis buffer (50 mM Tris-HCl, pH 7.5, 50 mM β-glycerophosphate, 150 mM NaCl, 10% glycerol, and 1% Tween 20, supplemented with protease and phosphatase inhibitors) for 1 h at 4°C. Insoluble components were removed by centrifugation at 16,000 *g* for 20 min at 4°C. For immunoprecipitations, 1 mg of total cell extract was precleared with 30 μl of protein G–Sepharose beads (GE Healthcare) for 3 h at 4°C. Senataxin was immunoprecipitated with 7.5 μg senataxin Ab-1 antibody overnight at 4°C. The following day, 40 μl of protein G–Sepharose beads was added for 1 h and incubated at 4°C. Immunoprecipitates were washed three times with lysis buffer and resuspended in 20 μl of sample loading buffer before separation of the proteins by SDS-PAGE. The proteins were then transferred onto a nitrocellulose membrane (Pall Life Sciences), and immunoblots were performed with the relevant antibodies.

Immunofluorescence

NFFs, AOA2 (SETX-1RM) fibroblasts, and HeLa were grown on glass coverslips for 48 h, washed with PBS, fixed in 2% paraformaldehyde/PBS for 10 min, and processed for immunofluorescence as previously described (Becherel et al., 2006) using the relevant antibodies, senataxin Ab-3 (1:400) and Ab-2 (1:200), RNA polymerase II (1:400; ab5408 [Abcam]), nucleolin (1:500; M019-3 [MBL International Corporation]), 3-nitrotyrosine (1:100; 9691 [Cell Signaling Technology]), 4-HNE-Michael adducts (1:100; 393207 [Calbiochem]). 8-oxo-dG was detected according to the manufacturer's protocol. Fluorochromes conjugated to the relevant secondary antibodies were Alexa Fluor 488 and 594 (Invitrogen). Images were captured using a digital camera (AxioCam MRm; Carl Zeiss MicroImaging, Inc.) attached to a fluorescent microscope (Axioskop2 mot plus; Carl Zeiss MicroImaging, Inc.) using Plan Apochromat 1.4 oil differential interference contrast (63× magnification). Imaging medium was PBS, and acquisition was performed at ambient temperature (25°C). AxioVision LE 4.3 software (Carl Zeiss MicroImaging, Inc.) was used to capture the individual images, which were assembled using Photoshop 7.0 (Adobe). Fluorescence intensity was quantitated on the RAW images using the public domain software ImageJ version 1.34s (NIH) before their assembly in Photoshop 7.0. After assembly, contrast was enhanced on all images simultaneously in Photoshop 7.0 using the brightness and contrast tool. No further image processing (e.g., surface or volume rendering, γ adjustment) was performed.

Analysis of DNA SSB repair

To induce SSB, cells were exposed to 20 μM H_2O_2 in RPMI 1640 medium without supplements for 15 min at 37°C. To remove H_2O_2, 880 U/ml catalase was added. Cells were collected by centrifugation (1,500 U/min for 5 min) and washed with PBSCMF (140 mM NaCl, 3 mM KCl, 8 mM Na_2HPO_4, and 1 mM KH_2PO_4). The numbers of SSBs were determined by an alkaline elution assay as previously described (Epe and Hegler, 1994). The numbers of SSBs in untreated control cells were subtracted in all cases. NAD(P)H depletion after H_2O_2 and MMS treatments was performed as previously described (Nakamura et al., 2003).

Repair kinetics of γH2AX foci

Cells were seeded onto coverslips, and experiments were performed on confluent fibroblasts. Cells were either irradiated or treated with H_2O_2 by adding 2 mM H_2O_2 into the growth medium for 10 or 30 min. Cells were washed with PBS and returned to fresh media. At the time points indicated, the cells were processed for immunofluorescence as described. Images were captured and assembled as described.

Online supplemental material

Fig. S1 shows characterization of mutations in two AOA2 cell lines. Fig. S2 shows characterization of senataxin antibodies. Fig. S3 shows induction of γH2AX foci in control (NFF) and AOA2 (SETX-1RM) cells after exposure to 2 mM H_2O_2. Fig. S4 shows complementation of the DNA DSB repair defect in AOA2 cells. The supplemental text gives primers used in this study. Online supplemental material is available at http://www.jcb.org/cgi/content/full/jcb.200701042/DC1.

We thank Aine Farrell for excellent cell culture assistance and Peter Parsons for the NFF strain.

This work is supported by the Australian National Health and Medical Research Council.

The authors declare that they have no conflict of interest.

Submitted: 8 January 2007
Accepted: 21 May 2007

Published June 11, 2007

References

Ahel, I., U. Rass, S.F. El-Khamisy, S. Katyal, P.M. Clements, P.J. McKinnon, K.W. Caldecott, and S.C. West. 2006. The neurodegenerative disease protein aprataxin resolves abortive DNA ligation intermediates. *Nature.* 443:713–716.

Aicardi, J., C. Barbosa, E. Andermann, F. Andermann, R. Morcos, Q. Ghanem, Y. Fukuyama, Y. Awaya, and P. Moe. 1988. Ataxia-ocular motor apraxia: a syndrome mimicking ataxia telangiectasia. *Ann. Neurol.* 24:497–502.

Bakkenist, C.J., and M.B. Kastan. 2003. DNA damage activates ATM through intermolecular autophosphorylation and dimer dissociation. *Nature.* 421:499–506.

Bar-Peled, M., and N.V. Raikhel. 1996. A method for isolation and purification of specific antibodies to a protein fused to the GST. *Anal. Biochem.* 241:140–142.

Barzilai, A., G. Rotman, and Y. Shiloh. 2002. ATM deficiency and oxidative stress: a new dimension of defective response to DNA damage. *DNA Repair (Amst.).* 1:3–25.

Becherel, O.J., N. Gueven, G.W. Birrell, V. Schreiber, A. Suraweera, B. Jakob, G. Taucher-Scholz, and M.F. Lavin. 2006. Nucleolar localization of aprataxin is dependent on interaction with nucleolin and on active ribosomal DNA transcription. *Hum. Mol. Genet.* 15:2239–2249.

Bouzyk, E., I. Gradzka, T. Iwanenko, M. Kruszewski, B. Sochanowicz, and I. Szumiel. 2000. The response of L5178Y lymphoma sublines to oxidative stress: antioxidant defence, iron content and nuclear translocation of the p65 subunit of NF-kappaB. *Acta Biochim. Pol.* 47:881–888.

Cantoni, O., P. Sestili, M. Fiorilli, M.P. Santoro, M.C. Tannoia, G. Novelli, F. Cattabeni, and B. Dallapiccola. 1989. Identification of 4 ataxia telangiectasia cell lines hypersensitive to gamma-irradiation but not to hydrogen peroxide. *Mutat. Res.* 218:143–148.

Cerosaletti, K., and P. Concannon. 2004. Independent roles for nibrin and Mre11-Rad50 in the activation and function of Atm. *J. Biol. Chem.* 279:38813–38819.

Chen, J.H., S.E. Ozanne, and C.N. Hales. 2005. Heterogeneity in premature senescence by oxidative stress correlates with differential DNA damage during the cell cycle. *DNA Repair (Amst.).* 4:1140–1148.

Chen, K., A. Albanp, A. Ho, and J.F. Keaney Jr. 2003. Activation of p53 by oxidative stress involves platelet-derived growth factor-beta receptor-mediated ataxia telangiectasia mutated (ATM) kinase activation. *J. Biol. Chem.* 278:39527–39533.

Chen, P.C., M.F. Lavin, C. Kidson, and D. Moss. 1978. Identification of ataxia telangiectasia heterozygotes, a cancer prone population. *Nature.* 274:484–486.

Chen, Y.Z., C.L. Bennett, H.M. Huynh, I.P. Blair, I. Puls, J. Irobi, I. Dierick, A. Abel, M.L. Kennerson, B.A. Rabin, et al. 2004. DNA/RNA helicase gene mutations in a form of juvenile amyotrophic lateral sclerosis (ALS4). *Am. J. Hum. Genet.* 74:1128–1135.

Chen, Y.Z., S.H. Hashemi, S.K. Anderson, Y. Huang, M.C. Moreira, D.R. Lynch, I.A. Glass, P.F. Chance, and C.L. Bennett. 2006. Senataxin, the yeast Sen1p orthologue: characterization of a unique protein in which recessive mutations cause ataxia and dominant mutations cause motor neuron disease. *Neurobiol. Dis.* 23:97–108.

Clements, P.M., C. Breslin, E.D. Deeks, P.J. Byrd, L. Ju, P. Bieganowski, C. Brenner, M.C. Moreira, A.M. Taylor, and K.W. Caldecott. 2004. The ataxia-oculomotor apraxia 1 gene product has a role distinct from ATM and interacts with the DNA strand break repair proteins XRCC1 and XRCC4. *DNA Repair (Amst.).* 3:1493–1502.

Cooke, M.S., N. Mistry, A. Ladapo, N.E. Herbert, and J. Lunec. 2000. Immunochemical quantitation of UV-induced oxidative and dimeric DNA damage to human keratinocytes. *Free Radic. Res.* 33:369–381.

Criscuolo, C., L. Chessa, S. Di Giandomenico, P. Mancini, F. Sacca, G.S. Grieco, M. Piane, F. Barbieri, G. De Michele, S. Banfi, et al. 2006. Ataxia with oculomotor apraxia type 2: a clinical, pathologic, and genetic study. *Neurology.* 66:1207–1210.

Dahm-Daphi, J., C. Sass, and W. Alberti. 2000. Comparison of biological effects of DNA damage induced by ionizing radiation and hydrogen peroxide in CHO cells. *Int. J. Radiat. Biol.* 76:67–75.

Date, H., O. Onodera, H. Tanaka, K. Iwabuchi, K. Uekawa, S. Igarashi, R. Koike, T. Hiroi, T. Yuassa, and Y. Awaya. 2001. Early onset ataxia with ocular motor apraxia and hypoalbuminemia is caused by mutations in a new HIT superfamily gene. *Nat. Genet.* 29:184–188.

Deschenes, F., L. Massip, C. Garand, and M. Lebel. 2005. In vivo misregulation of genes involved in apoptosis, development and oxidative stress in mice lacking both functional Werner syndrome protein and poly(ADP-ribose) polymerase-1. *Hum. Mol. Genet.* 14:3293–3308.

Duquette, A., K. Roddier, J. McNabb-Baltar, I. Gosselin, A. St-Denis, M.J. Dicaire, L. Loisel, D. Labuda, L. Marchand, J. Mathieu, et al. 2005. Mutations in senataxin responsible for Quebec cluster of ataxia with neuropathy. *Ann. Neurol.* 57:408–414.

Epe, B., and J. Hegler. 1994. Oxidative DNA damage: endonuclease fingerprinting. *Methods Enzymol.* 234:122–131.

Gorbalenya, A.E., E.V. Koonin, A.P. Donchenko, and V.M. Blinov. 1989. Two related superfamilies of putative helicases involved in replication, recombination, repair and expression of DNA and RNA genomes. *Nucleic Acids Res.* 17:4713–4730.

Grohmann, K., M. Schuelke, A. Diers, K. Hoffmann, B. Lucke, C. Adams, E. Bertini, H. Leonhardt-Horti, F. Muntoni, R. Ouvrier, et al. 2001. Mutations in the gene encoding immunoglobulin mu-binding protein 2 cause spinal muscular atrophy with respiratory distress type 1. *Nat. Genet.* 29:75–77.

Gueven, N., O.J. Becherel, A.W. Kijas, P. Chen, O. Howe, J.H. Rudolph, R. Gatti, H. Date, O. Onodera, G. Taucher-Scholz, and M.F. Lavin. 2004. Aprataxin, a novel protein that protects against genotoxic stress. *Hum. Mol. Genet.* 13:1081–1093.

Gueven, N., P. Chen, J. Nakamura, O.J. Becherel, A.W. Kijas, P. Grattan-Smith, and M.F. Lavin. 2007. A subgroup of spinocerebellar ataxias defective in DNA damage response. *Neuroscience.* 145:1418–1425.

Gustafson, D.L., H.R. Franz, A.M. Ueno, C.J. Smith, D.J. Doolittle, and C.A. Waldren. 2000. Vanillin (3-methoxy-4-hydroxybenzaldehyde) inhibits mutation induced by hydrogen peroxide, N-methyl-N-nitrosoguanidine and mitomycin C but not (137)Cs gamma-radiation at the CD59 locus in human-hamster hybrid A(L) cells. *Mutagenesis.* 15:207–213.

Hayashi, M., M. Itoh, S. Araki, S. Kumada, K. Shioda, K. Tamagawa, T. Mizutani, Y. Morimatsu, M. Minagawa, and M. Oda. 2001. Oxidative stress and disturbed glutamate transport in hereditary nucleotide repair disorders. *J. Neuropathol. Exp. Neurol.* 60:350–356.

Hernandez, D., C.M. McConville, M. Stacey, C.G. Woods, M.M. Brown, P. Shutt, G. Rysiecki, and A.M. Taylor. 1993. A family showing no evidence of linkage between the ataxia telangiectasia gene and chromosome 11q22-23. *J. Med. Genet.* 30:135–140.

Hickson, I.D. 2003. RecQ helicases: caretakers of the genome. *Nat. Rev. Cancer.* 3:169–178.

Hoffmann, S., D. Spitkovsky, J.P. Radicella, B. Epe, and R.J. Wiesner. 2004. Reactive oxygen species derived from the mitochondrial respiratory chain are not responsible for the basal levels of oxidative base modifications observed in nuclear DNA of mammalian cells. *Free Radic. Biol. Med.* 36:765–773.

Ismail, I.H., S. Nystrom, J. Nygren, and O. Hammarsten. 2005. Activation of ataxia telangiectasia mutated by DNA strand break-inducing agents correlates closely with the number of DNA double strand breaks. *J. Biol. Chem.* 280:4649–4655.

Kozlov, S.V., M.E. Graham, C. Peng, P. Chen, P.J. Robinson, and M.F. Lavin. 2006. Involvement of novel autophosphorylation sites in ATM activation. *EMBO J.* 25:3504–3514.

Kurz, E.U., and S.P. Lees-Miller. 2004. DNA damage-induced activation of ATM and ATM-dependent signalling pathways. *DNA Repair (Amst.).* 3:889–900.

Lavin, M.F., and Y. Shiloh. 1997. The genetic defect in ataxia-telangiectasia. *Annu. Rev. Immunol.* 15:177–202.

Le Ber, I., M.C. Moreira, S. Rivaud-Pechoux, C. Chamayou, F. Ochsner, T. Kuntzer, M. Tardieu, G. Said, M.O. Habert, G. Demarquay, et al. 2003. Cerebellar ataxia with oculomotor apraxia type 1: clinical and genetic studies. *Brain.* 126:2761–2772.

Le Ber, I., A. Brice, and A. Durr. 2005. New autosomal recessive cerebellar ataxias with oculomotor apraxia. *Curr. Neurol. Neurosci. Rep.* 5:411–417.

Lee, J.H., and T.T. Paull. 2005. ATM activation by DNA double-strand breaks through the Mre11-Rad50-Nbs1 complex. *Science.* 308:551–554.

Letavayova, L., E. Markova, K. Hermanska, V. Vlckova, D. Vlasakova, M. Chovanec, and J. Brozmanova. 2006. Relative contribution of homologous recombination and non-homologous end-joining to DNA double-strand break repair after oxidative stress in *Saccharomyces cerevisiae*. *DNA Repair (Amst.).* 5:602–610.

Li, Y., H. Zhu, and M.A. Trush. 1999. Detection of mitochondria-derived reactive oxygen species production by the chemilumingenic probes lucigenin and luminol. *Biochim. Biophys. Acta.* 1428:1–12.

Moreira, M.C., C. Barbot, N. Tachi, N. Kozuka, E. Uchida, T. Gibson, P. Mendonca, M. Costa, J. Barros, T. Yanagisawa, et al. 2001. The gene mutated in ataxia-ocular apraxia 1 encodes the new HIT/Zn-finger protein aprataxin. *Nat. Genet.* 29:189–193.

Moreira, M.C., S. Klur, M. Watanabe, A.H. Nemeth, I. Le Ber, J.C. Moniz, C. Tranchant, P. Aubourg, M. Tazir, L. Schols, et al. 2004. Senataxin, the ortholog of a yeast RNA helicase, is mutant in ataxia-ocular apraxia 2. *Nat. Genet.* 36:225–227.

Mosesso, P., M. Piane, F. Palitti, G. Pepe, S. Penna, and L. Chessa. 2005. The novel human gene aprataxin is directly involved in DNA single-strand break repair. *Cell. Mol. Life Sci.* 62:485–491.

Published June 11, 2007

Nakamura, J., S. Asakura, S.D. Hester, G. de Murcia, K.W. Caldecott, and J.A. Swenberg. 2003. Quantitation of intracellular NAD(P)H can monitor an imbalance of DNA single strand break repair in base excision repair deficient cells in real time. *Nucleic Acids Res.* 31:e104.

Nemeth, A.H., E. Bochukova, E. Dunne, S.M. Huson, J. Elston, M.A. Hannan, M. Jackson, C.J. Chapman, and A.M. Taylor. 2000. Autosomal recessive cerebellar ataxia with oculomotor apraxia (ataxia-telangiectasia-like syndrome) is linked to chromosome 9q34. *Am. J. Hum. Genet.* 67:1320–1326.

Pagano, G., A. Zatterale, P. Degan, M. d'Ischia, F.J. Kelly, F.V. Pallardo, and S. Kodama. 2005. Multiple involvement of oxidative stress in Werner syndrome phenotype. *Biogerontology.* 6:233–243.

Riballo, E., M. Kuhne, N. Rief, A. Doherty, G.C. Smith, M.J.M.J. Recio, C. Reis, K. Dahm, A. Fricke, A. Krempler, et al. 2004. A pathway of double-strand break rejoining dependent upon ATM, Artemis, and proteins locating to gamma-H2AX foci. *Mol. Cell.* 16:715–724.

Rothkamm, K., and M. Lobrich. 2003. Evidence for a lack of DNA double-strand break repair in human cells exposed to very low x-ray doses. *Proc. Natl. Acad. Sci. USA.* 100:5057–5062.

Scherl, A., Y. Coute, A. Calle, K. Kindbeiter, J.C. Sanchez, A. Greco, D. Hochstrasser, and J.J. Diaz. 2002. Functional proteomic analysis of human nucleolus. *Mol. Biol. Cell.* 13:4100–4109.

Steinmetz, E.J., C.L. Warren, J.N. Kuehner, B. Panbehi, A.Z. Ansari, and D.A. Brow. 2006. Genome-wide distribution of yeast RNA polymerase II and its control by Sen1 helicase. *Mol. Cell.* 24:735–746.

Stewart, G.S., R.S. Maser, T. Stankovic, D.A. Bressan, M.I. Kaplan, N.G. Jaspers, A. Raams, P.J. Byrd, J.H. Petrini, and A.M. Taylor. 1999. The DNA double-strand break repair gene hMRE11 is mutated in individuals with an ataxia-telangiectasia-like disorder. *Cell.* 99:577–587.

Stucki, M., and S.P. Jackson. 2006. γH2AX and MDC1: anchoring the DNA-damage-response machinery to broken chromosomes. *DNA Repair (Amst.).* 5:534–543.

Suzuki, M., K. Suzuki, S. Kodama, and M. Watanabe. 2006. Phosphorylated histone H2AX foci persist on rejoined mitotic chromosomes in normal human diploid cells exposed to ionizing radiation. *Radiat. Res.* 165:269–276.

Szekely, A.M., F. Bleichert, A. Numann, S. Van Komen, E. Manasanch, A. Ben Nasr, A. Canaan, and S.M. Weissman. 2005. Werner protein protects nonproliferating cells from oxidative DNA damage. *Mol. Cell. Biol.* 25:10492–10506.

Taylor, A.M., D.G. Harnden, C.F. Arlett, S.A. Harcourt, A.R. Lehmann, S. Stevens, and B.A. Bridges. 1975. Ataxia telangiectasia: a human mutation with abnormal radiation sensitivity. *Nature.* 258:427–429.

Taylor, A.M., A. Groom, and P.J. Byrd. 2004. Ataxia-telangiectasia-like disorder (ATLD)—its clinical presentation and molecular basis. *DNA Repair (Amst.).* 3:1219–1225.

Toiber, D., and H. Soreq. 2005. Cellular stress reactions as putative cholinergic links in Alzheimer's disease. *Neurochem. Res.* 30:909–919.

Ursic, D., K.L. Himmel, K.A. Gurley, F. Webb, and M.R. Culbertson. 1997. The yeast SEN1 gene is required for the processing of diverse RNA classes. *Nucleic Acids Res.* 25:4778–4785.

Ursic, D., K. Chinchilla, J.S. Finkel, and M.R. Culbertson. 2004. Multiple protein/protein and protein/RNA interactions suggest roles for yeast DNA/RNA helicase Sen1p in transcription, transcription-coupled DNA repair and RNA processing. *Nucleic Acids Res.* 32:2441–2452.

Uziel, T., Y. Lerenthal, L. Moyal, Y. Andegeko, L. Mittelman, and Y. Shiloh. 2003. Requirement of the MRN complex for ATM activation by DNA damage. *EMBO J.* 22:5612–5621.

Wallace, S.S. 2002. Biological consequences of free radical-damaged DNA bases. *Free Radic. Biol. Med.* 33:1–14.

Weng, Y., K. Czaplinski, and S.W. Peltz. 1996. Genetic and biochemical characterization of mutations in the ATPase and helicase regions of the Upf1 protein. *Mol. Cell. Biol.* 16:5477–5490.

Werner, S.R., A.K. Prahalad, J. Yang, and J.M. Hock. 2006. RECQL4-deficient cells are hypersensitive to oxidative stress/damage: insights for osteosarcoma prevalence and heterogeneity in Rothmund-Thomson syndrome. *Biochem. Biophys. Res. Commun.* 345:403–409.

Wharton, W. 1995. Cell cycle constraints on peroxide- and radiation-induced inhibitory checkpoints. *Cancer Res.* 55:5069–5074.

Zhang, N., P. Chen, K.K. Khanna, S. Scott, M. Gatei, S. Kozlov, D. Watters, K. Spring, T. Yen, and M.F. Lavin. 1997. Isolation of full-length ATM cDNA and correction of the ataxia telangiectasia cellular phenotype. *Proc. Natl. Acad. Sci. USA.* 94:8021–8026.